SAND2018-5515C

Comparative Review of High Resolution Monitoring Versus Standard Inverter Data Acquisition for a Single Photovoltaic Power Plant

C. Birk Jones *, Benjamin H. Ellis †, Joshua S. Stein *and Joseph Walters ‡

*Sandia National Laboratories, Albuquerque, NM, U.S.A
† Lawrence Berkeley National Laboratory, Berkeley, CA, U.S.A
‡Florida Solar Energy Center, Cocoa, FL, U.S.A

***Abstract*—Investing in data monitoring equipment will provide help ensure that the PV array is operating as expected. The systems can be designed to limit extensive downtime that would result in lost revenue. New, higher resolution systems can also be used to quantify performance using detailed characterization techniques. The Pordis 140A system can extract current and voltage (I-V) while the PV system remains connected to the grid. The added visibility for plant owners, investors, and operators is currently not well understood. Therefore, the present work provides an overview of the I-V tracing system in comparison to a typical, inverter data acquisition system for two systems located in Albuquerque, New Mexico. The review includes a description of basic energy yield calculations, degradation analysis, and abnormal behavior diagnostics.**

***Index Terms*—photovoltaic monitoring**

I. Introduction

Solar photovoltaic (PV) monitoring systems have been a valuable tool for owners, investors, installers, and operators to verify that plants are operating as expected [1]. This includes continuous, real-time monitoring and PV plant commissioning [2]. The design and installation of data monitoring systems includes a site survey, definition of monitored data and graphical interface, review of monitoring equipment power requirements, and specifications of data communications circuits. The intent has been to create a systems that helps avoid extensive downtime [3].

Typical PV systems have relied on maximum power point data acquisition (DAQ) systems instead of more advanced high resolution devices to monitor system health. The conventional monitoring systems have been used to sense DC and AC current, voltage, and maximum power. Where as, high resolution monitoring systems, available on the market today, can provide in situ current and voltage (I-V) curves. The high resolution monitoring does require more upfront investment and as of yet system owners have not jumped at the opportunity to install more advanced systems. The advantages of the in situ I-V curve tracing systems have not yet been clearly defined to help justify the investment.

The present work compares the output from an inverter DAQ system and an in situ string level I-V curve tracing device connected to two systems in Albuquerque, New Mexico. The evaluation of the typical and non-typical data monitoring approaches considered the review of energy yield, degradation, and characterization of abnormal performance. The system yield and performance ratio have been a convenient, yet elementary way to evaluate energy production of PV systems [4]. The analysis of degradation can be performed using power only [5][6], but I-V curves are required to define the specific degradation mechanism. The curves provide a detailed representation of system performance that can be used to quickly detect and diagnose abnormal system behavior. The paper provides an overview of the methodology in Section II, the results are described in Section III, and the final concluding remarks are in Section IV.

II. Methodology

Solar PV owners and operators, concerned with long-term operations, monitor energy output, degradation, and abnormal activity. The monitoring of these aspects have been performed with conventional monitoring systems that track the maximum power point (MPP) power, current, and voltage. New, more expensive monitoring systems are now available and provide higher resolution performance characterization. The advanced characterization of PV array sub-systems can now be monitored using in situ I-V curve tracing devices. However, it is not yet clear if the extra cost will improve the long-term performance of the system. Detailed analysis of the integration strategies and specific benefits should be explored to provide a clear understanding. This paper provides a first step review of the potential differences that is based on a basic overview of the two monitoring approaches on a single PV power plant.

Fig. 1. The solar photovoltaic array was located in Albuquerque, New Mexico. It included two inverters that each supported four strings. The eight strings were routed to a Pordis I-V curve tracing system prior to the combiner box. The combined strings were monitored using the inverters data acquisition system.

Sandia National Laboratories is a multimission laboratory managed and operated by National Technology & Engineering Solutions of Sandia, LLC, a wholly owned subsidiary of Honeywell International Inc., for the U.S. Department of Energy's National Nuclear Security Administration under contract DE-NA0003525.

A. Photovoltaic Solar Array

The comparative analysis of high resolution and typical monitoring systems used two PV systems located in Albuquerque, New Mexico (Figure 1). A single system was defined by the number of inverters, and in this case 8 strings were connected to two inverters. The first system was comprised of four strings labeled as 1A, 1B, 2A, and 2B as shown in Figure 2. The second system also had four strings that were labeled as 3A, 3B, 4A, and 4B. Each of the strings was comprised of 14 modules that had an Standard Test Condition (STC) rated power output of 260 Watts for a total of 3641 Watts and 3644 Watts total power ratting for the first and second systems respectively. The two systems had two different module manufactures and were connected to their own inverters that were the same make and model. The

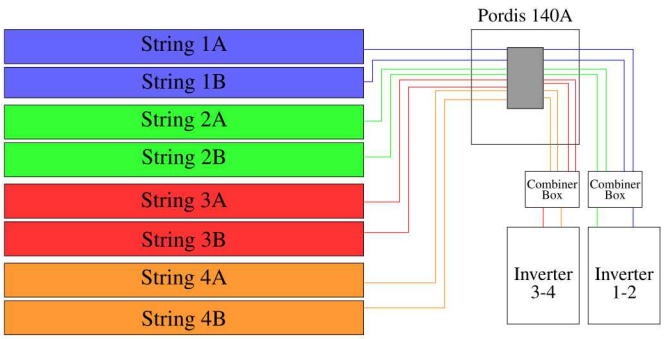

Fig. 2. The eight strings of the two test arrays connected to the Pordis I-V Characterization System and then to the combiner box before connecting to the inverter. Strings 1A, 1B, 2A, and 2B were comprised of modules that were different than 3A, 3B, 4A, and 4B strings.

available ports in the inverters required that the A and B strings be combined prior to entering their respective inverters. The combination of the A and B strings for the two systems meant that the conventional monitoring system was not able to sense current and voltage at the string level.

B. Conventional Monitoring

The conventional monitoring system used in the present work was provided by the inverter manufacturer. The two

Fig. 3. The conventional monitoring system was performed by the off-the-shelf inverter product called the Cluster Controller. The Cluster Controller connected to each of the two inverters and aggregated each of the systems data into a centralized location.

SMA inverters were connected to a *Cluster Controller* device shown in Figure 3. The devices aggregated the data from each of the inverters and provided a visual interface and a ftp connection to collect performance data in xml or csv format. The *cluster controller* provided time-series data in 5 minute intervals. The data was accessed each day by the research team and stored in the same database as the high resolution monitoring data.

C. High Resolution Monitoring

The Porids 140A high resolution monitoring system (Figure 4) was used to collect string level I-V curves at 30 minute intervals for each string. The system was connected in-between the PV modules and the combiner box as shown in Figure 2. The 140A was designed as an in situ tracer, which means that it may remain connected to the array at all times without impacting normal operations. The I-V tracing process began with the isolation of a string from the array, the string was redirected to the load portion of the device, an I-V trace was performed, and then the string was switched back into the array. This process took about 100ms to complete. Additionally,

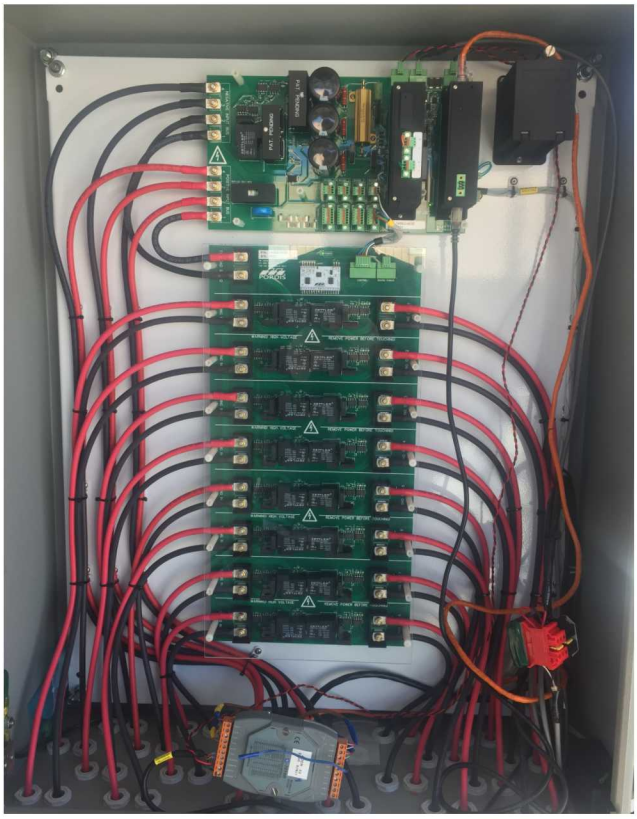

Fig. 4.

the switch circuitry did not trip the high-frequency arc fault detection nor the ground fault detection of the inverter. The results from each of the string I-V traces were stored in a database located in the tracer system and were routed to the central database for analysis.

D. Comparative Analysis

The present work compared the outputs of a typical monitoring system provided by most inverter manufactures with the Pordis high resolution monitoring system that periodically performed I-V sweeps for each of the eight strings. The comparison included a review of the:

1) calculated energy yield,
2) extent of the degradation analysis, and
3) identification of abnormal behavior for each approach.

The three componenbts are important for monitoring long-term system health. The calculated energy yield can be computed on a daily, monthly, and annual basis to provide a high level evaluation of PV system performance. The degradation analysis has been used to track the durability of the system and confirm warranty concerns. And, abnormal behavior or fault conditions can be identified using monitoring systems to avoid tracker control issues, excessive hot spots, mismatch problems, and other string level mishaps. There are many methods for calculating degradation and this paper attempted to replicate a common approach.

The present work removed the seasonal impacts from the data to evaluate degradation by performing two types of conversions. The first approach, applied to the maximum power point data, was the Power Performance Index (PPI) [7]. The I-V curve data was converted to STC before it's degradation was evaluated. The PPI was used to normalize the data by dividing the measured power ($P_{measured}$) by the modeled power ($P_{modeled}$) output. $P_{modeled}$ was calculated using the California Energy Commission (CEC) model. The CEC model is based on the electrical representation of the PV module defined by the single diode equivalent circuit [8]. The STC conversion was performed using translation equations defined by Anderson [9]:

$$I_{\text{stc,curve}} = \frac{I_{\text{meas.,curve}}}{(1+\alpha_{I_{sc}}(T_m-25)(E/1000))} \tag{1}$$

$$V_{\text{stc,curve}} = \frac{V_{\text{meas.,curve}}}{(1+\beta_{V_{oc}}(T_m-25)(1+\delta\ln(E/1000)))} \tag{2}$$

The variables in Equations 1 and 2 that calculate the STC current and voltage are defined as:

- $\alpha_{I_{sc}}$ is the short circuit current temperature coefficient,
- $\beta_{V_{oc}}$ is the open circuit temperature coefficient,
- T_m is the measured module temperature,
- E is the measured solar irradiance,
- $I_{\text{meas.,curve}}$ is the measured I-V curve current, and
- $V_{\text{meas.,curve}}$ is the measured I-V curve voltage.

III. Results

The results for the comparative analysis review the energy yield, degradation, and abnormal performance identification for the two monitoring methodologies.

A. Energy Yield

The two approaches each measured the instantaneous maximum power. The conventional approach collected the maximum power that was discovered by the inverter controls algorithm. In some cases, the inverter may not find the maximum

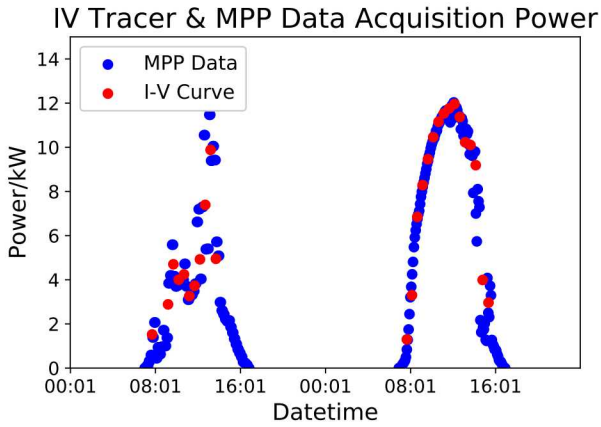

Fig. 5. The MPP data acquisition system collected data at 5 minute intervals and the I-V tracer performed sweeps every 30 minutes.

power point because of mismatch or bad seeking algorithm. Whereas, the I-V tracing system discovered the theoretical maximum based on the measured I-V curve. The results for each approach over a two day period are shown in Figure 5. The I-V curve data produced more scattered results compared to the consistent 5 minute data collection provided by the MPP data set. The scattered data collection of the I-V curve tracing

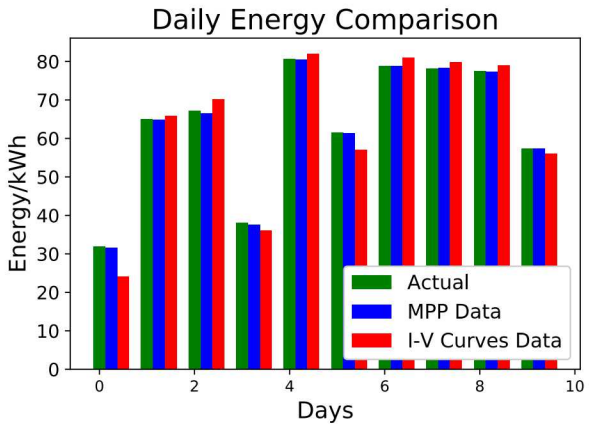

Fig. 6. The daily energy was computed using the two approaches and the MPP data acquisition system had smaller errors than the I-V tracing system.

system caused the accumulated energy to not be as accurate as the MPP data set as shown Figure 6 that plots the daily energy for each approach. The cumulative error over the 10 day period plotted in Figure 6 was much higher for the I-V curve data compared to the MPP data. The absolute error, plotted in Figure 7, went over 25kWh for the I-V curve data and did not reach above 5kWh for the MPP data over the 10 day period.

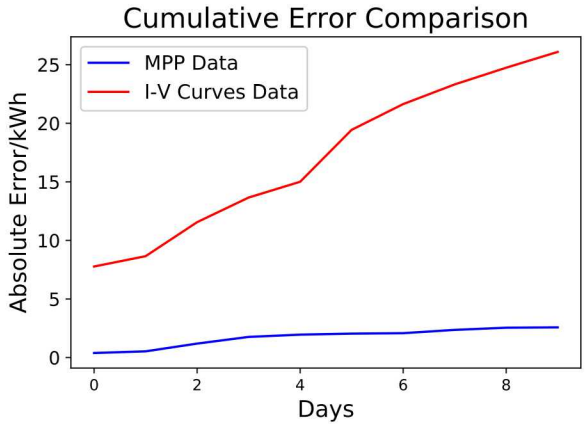

Fig. 7. The absolute cumulative error was just over 5 times higher for the I-V curve data compared to the MPP data.

B. Degradation

The degradation of the eight strings was evaluated using the data from the two monitoring systems. The typical approach, that used the MPP data, was only able to evaluate the degradation of the combined strings as shown in Figure 8. It was evident that the modules in strings 1A, 1B, 2A, and 2B performed differently than the modules in strings 3A, 3B, 4A, and 4B. Also, strings 3A-B began at a performance level that was considerably lower than the expected model output. The

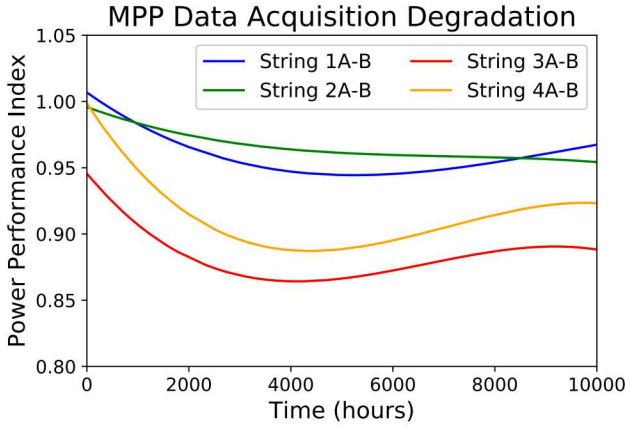

Fig. 8. Power performance index for the combined strings over a 60 week period showed that strings 3A-B and 4A-B degraded by about 10%. Strings 1A-B and 2A-B degradation was about 5%.

I -V tracing system, on the other hand, was able to evaluate all of the strings and analyze numerous module characteristics. For example, the I -V curve system was used to monitor short circuit and open circuit voltage changes over time as shown in Figure 9, and 10.

The detailed analysis of the I -V curve data stepped beyond the MPP data set and provided a means to define the mechanism for the string level degradation. For instance, the data provided evidence that strings 3A and 3B were under performing because both the voltage and current were low. In this case, the reduction in power was not caused by extra series resistance or a reduction in shunt resistance but instead an overall drop in both voltage and current. This conclusion was evident in the Fill Factor (FF) ratios plotted in Figures 11 - 13, where the current and voltage ratios were not low and actual outperformed the other strings. The FF, defined by

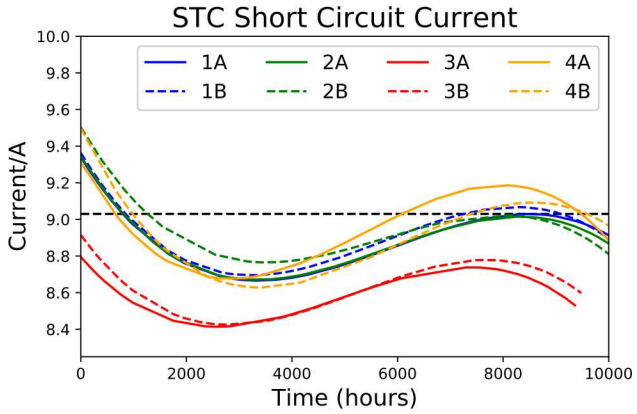

Fig. 9. Each of the strings calculated STC short circuit current decreased from hour zero to about hour 3,200. The current then increased and showed signs of leveling off around the rated current value. Strings 3A and 3B, however, did not reach the rated value and leveled off at a value that was 3.5% below.

Equation 3, provides a general overview of the I-V curve characteristics. The maximum power point current (I_{mp}) and short circuit current (I_{sc}) ratio provides a basic review of the shunt resistance. And, maximum power point voltage (V_{mp})

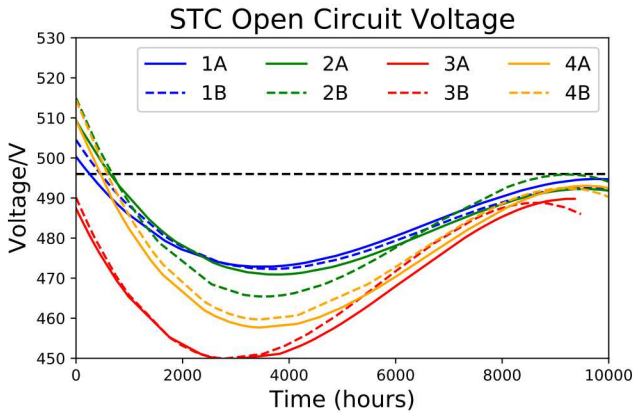

Fig. 10. The open circuit voltage at STC tended to drop from the beginning of life until about hour 3,500. The voltage then increased to the rated value and leveled off.

and open circuit voltage (V_{oc}) ratio helps define the series resistance. If the ratios were close to one, than the shunt and series resistance may not be impacting performance. However, if the ratios are low than the resistance components may be impacting the modules power output.

$$\text{Fill Factor} = \frac{(I_{mp})(V_{mp})}{(I_{sc})(V_{oc})} \tag{3}$$

Even though strings 4A and 4B were comprised of the same make and model, and were connected to the same inverter as 3A and 3B they tended to have a higher power

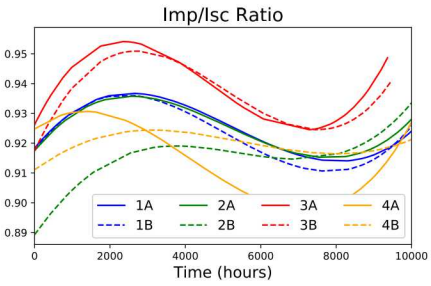

Fig. 11. The I_{mp}/I_{sc} ratio provides a basic review of the shunt resistance over time.

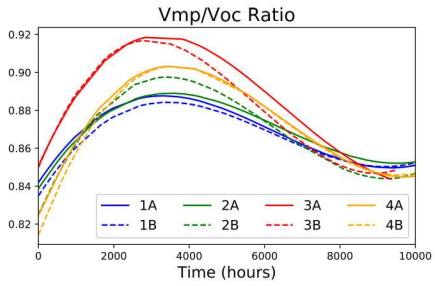

Fig. 12. The V_{mp}/V_{sc} ratio describes the series resistance associated with the PV string.

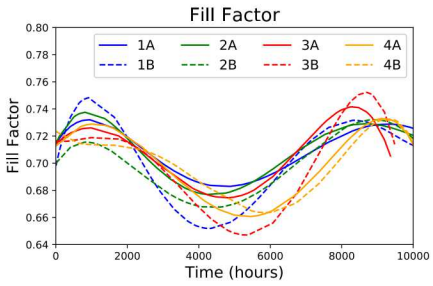

Fig. 13. The calculate fill factor is the ratio of maximum power to the product of I_{sc} and V_{oc}.

output. However, each of the strings tended to have a similar degradation rate between hour zero and 3,500. Strings 4A and 4B showed signs of shunt resistance issues that caused I_{mp} to decrease at a higher rate compared to I_{sc} as indicated by reviewing the I_{sc} (Figre 9) and I_{mp}/I_{sc} ratio (Figure 11) trends together.

According to the MPP data degradation analysis strings 2A and 2B did not degrade as significantly as the others. The degradation plot, based on PPI, in Figure 8 did not capture the full story. String 2B, which was absorbed into the MPP data analysis because it was combined with 2A, showed signs of shunt resistance degradation issues that caused that caused I_{mp} to degrade at a faster rate than string 2A. The extra analysis provided by the I-V curve data set led to a more detailed review of system performance and characteristic changes over time.

C. Abnormal Performance

Any abnormal sub-system performance was difficult to identify using inverter level monitoring. For example, end of the day shading caused by low sun angle and nearby fences was not clear in the DC power as shown in the left side of Figure 14. However, the string level mismatch at that time of

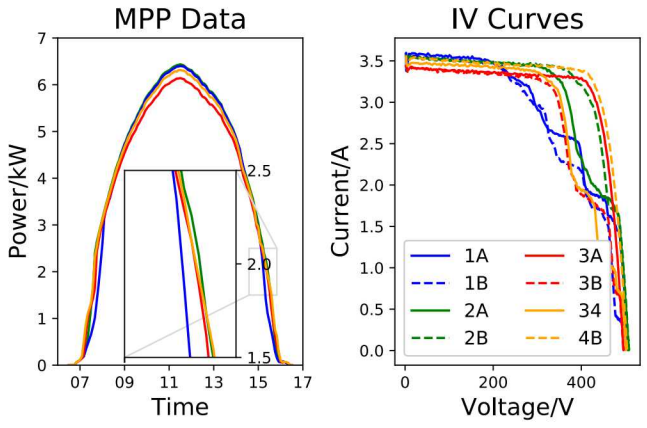

Fig. 14. The end of the day shading was difficult to notice in the maximum power point data provided by the inverter. It was clear in the string level I-V curves.

day was evident in the I-V curves as shown in the right side of Figure 14. The mismatch condition was a result of shading that was caused by a fence located to the south west of the array.

Mismatch refers to the power losses of the PV string associated with the interconnection of modules that have different electrical properties or outputs. As a result of mismatch, a

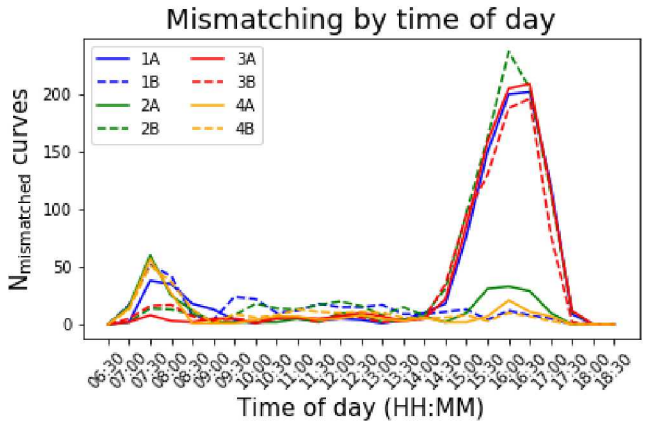

Fig. 15. Number of curves at every half hour of the day for each string where mismatch was detected.

non-ideal I-V curve is generated that causes the maximum power point operating point to decrease. The non-ideal I-V curve will have one or more inflection points that could shift the maximum power point to a lower voltage as shown on the right plot in Figure 14. The identification of mismatch could provide operators with valuable information regarding the state of the tracking system, extensive module damage caused by hot spots, and other issues. The identification of the mismatch behavior was performed and used to evaluate the health of the system.

The detection algorithm, used in this work, identified potential mismatch by evaluating where the derivative changed. The results for three different I-V curves are highlighted in Figures 16 - 18. The mismatch occurrences were then accumulated and grouped by time of day over the course of the monitoring process as shown in Figure 15. The largest number of mismatch events occurred at the start and end of the day. The strings most effected by mismatch where 1A, 2B, 3A, and 3B. Strings 3A and 3B, which were the worst

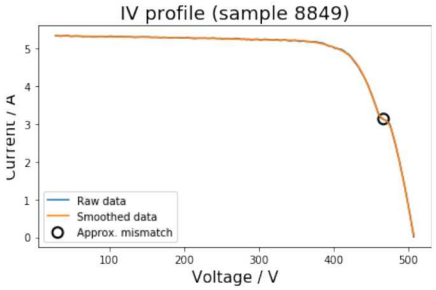

Fig. 16. I-V curve with one inflection point caused by a mismatch condition was identified by the detection algorithm.

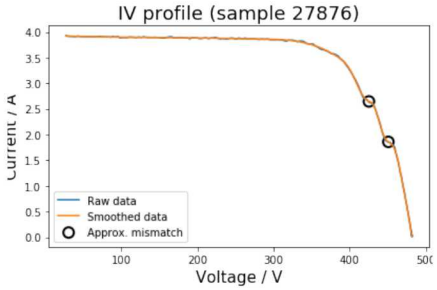

Fig. 17. Two inflection points were detected, which implied that multiple mismatch conditions had occurred.

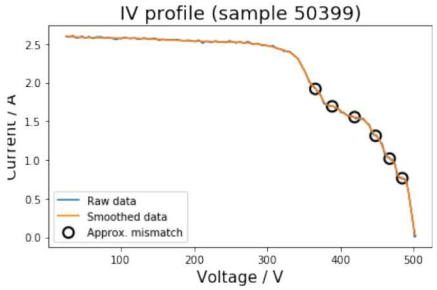

Fig. 18. The I-V curve had multiple inflection points, which signaled that the string was experiencing significant mismatch.

performing strings, had almost 1.5 times as many curves with mismatch as the curves with minimal mismatch impacts (1B, 2A, 4A, and 4B) as shown in Figure 19.

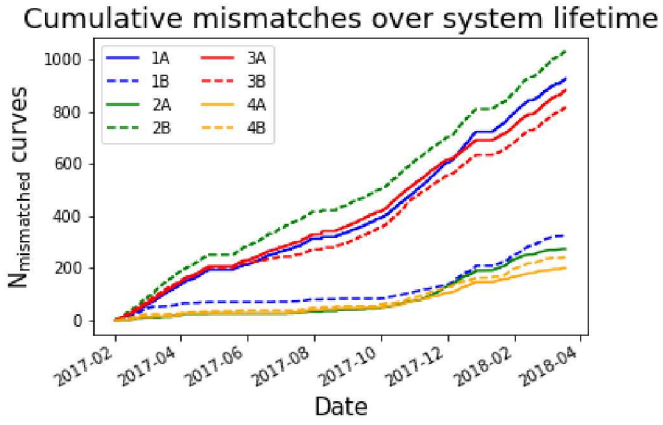

Fig. 19. Cumulative number of curves with mismatch detected over the systems lifetime.

IV. Conclusion

The present work compared the outputs of conventional monitoring (MPP data) with a high resolution (I-V curve data) system. The MPP system was able to approximate energy generation better, but the I-V curves provided a more detailed review of degradation and abnormal conditions. The I-V curve data allowed for the specific strings to be identified, and through detailed analysis the distinct degradation mechanisms could be defined. Abnormal performance was difficult to disaggregate in the MPP data. The I-V curve data provided a detailed characterization of the sub-system health that defined shunt and series resistance, mismatch conditions, and other issues. This paper provided a basic overview of the two approaches and the next step is to perform a detailed analysis that includes specific fault or degradation conditions, and considers the investment opportunity. In order to justify the extra cost of the I-V curve tracing device a detailed cost analysis should be performed.

References

[1] K. Moore and R. Hren, "Commercial PV System Data Monitoring, Part One," *SolarPro Magazine*, no. 4.6, Nov. 2011. [Online]. Available: /articles/products-equipment/monitoring/commercial-pv-system-data-monitoring-part-one

[2] B. Gleason, "PV System Commissioning," *SolarPro Magazine*, no. 2.6, Nov. 2009. [Online]. Available: /articles/design-installation/pv-system-commissioning

[3] K. Moore and H. Rebekah, "Commercial PV System Data Monitoring, Part Two," *SolarPro Magazine*, no. 5.1, Jan. 2012. [Online]. Available: /articles/products-equipment/monitoring/commercial-pv-system-data-monitoring-part-two

[4] B. Marion, J. Adelstein, K. Boyle, H. Hayden, B. Hammond, T. Fletcher, B. Canada, D. Narang, A. Kimber, L. Mitchell, G. Rich, and T. Townsend, "Performance parameters for grid-connected PV systems," in *Conference Record of the Thirty-first IEEE Photovoltaic Specialists Conference, 2005.*, Jan. 2005, pp. 1601–1606.

[5] D. C. Jordan, R. M. Smith, C. R. Osterwald, E. Gelak, and S. R. Kurtz, "Outdoor PV degradation comparison," in *2010 35th IEEE Photovoltaic Specialists Conference*, Jun. 2010, pp. 002 694–002 697.

[6] D. C. Jordan and S. R. Kurtz, "Analytical improvements in PV degradation rate determination," in *2010 35th IEEE Photovoltaic Specialists Conference*, Jun. 2010, pp. 002 688–002 693.

[7] T. Townsend, C. Whitaker, B. Farmer, and H. Wenger, "A new performance index for PV system analysis," in *Proceedings of 1994 IEEE 1st World Conference on Photovoltaic Energy Conversion - WCPEC (A Joint Conference of PVSC, PVSEC and PSEC)*, vol. 1, Dec. 1994, pp. 1036–1039 vol.1.

[8] W. De Soto, S. A. Klein, and W. A. Beckman, "Improvement and validation of a model for photovoltaic array performance," *Solar Energy*, vol. 80, no. 1, pp. 78–88, Jan. 2006. [Online]. Available: http://www.sciencedirect.com/science/article/pii/S0038092X05002410

[9] A. Anderson, "PV translation equations a new approach," vol. 353, Jan. 1996.

Acknowledgments

This material is based upon work supported by the U.S. Department of Energy's Office of Energy Efficiency and Renewable Energy (EERE) under the Solar Energy Technology Office, Award Number DE-EE0008157.

Sandia National Laboratories is a multimission laboratory managed and operated by National Technology and Engineering Solutions of Sandia, LLC., a wholly owned subsidiary of Honeywell International, Inc., for the U.S. Department of Energy's National Nuclear Security Administration under contract DE-NA0003525.